Alan Salari and Danilo Erricolo

Unmanned Aerial Vehicles for High-Frequency Measurements

An accurate, fast, and cost-effective technology.

The use of unmanned aerial vehicles (UAVs) for high-frequency (HF) measurements is a cutting-edge technology that has recently attracted attention. The measurements of far and near fields of antennas, mobile network tests, direction finding, and locating the sources of interference as well as radio-frequency (RF) imaging are a few of the HF applications of UAVs. In this article, we discuss the advantages and capabilities of UAVs for HF measurements as well as some recent progress in the use of UAVs for related types of applications.

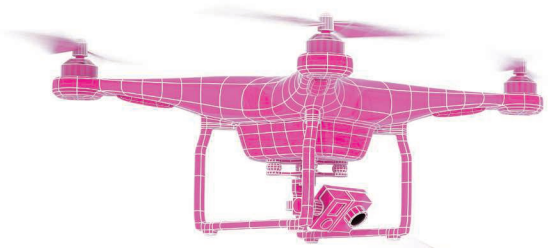

©SHUTTERSTOCK.COM/ORANGE DEER STUDIO

Digital Object Identifier 10.1109/MAP.2021.3061026
Date of current version: 12 May 2021

INTRODUCTION

UAVs, or drones, are used for different applications, from surveillance, delivery, and search and rescue to smart farming, inspection, filming, streaming, and advanced imaging [1]–[11]. They can also be controlled in groups to fulfill certain specialized missions [12], [13]. UAVs are very appealing due to their low-cost, high maneuverability, and most importantly, their ability to access hard-to-reach positions. Using UAVs has opened new avenues for more efficient data collection, enabling smarter decisions, optimized processes, and significantly reduced amounts of time and money. Many industries use drones, but the three fastest-growing commercial sectors in 2018 were construction, mining, and agriculture with a 239, 198, and 172% growth, respectively, in using UAVs [14]. Based on another report [15], the global drone market is expected grow from US$14 billion in 2018 to US$43 billion in 2024.

UAVs have recently been used for HF measurements such as mobile network testing, measurements of the far and near fields of antennas [16]–[19], direction finding, and RF imaging [20]. The main advantage of UAVs is their capability to perform measurements in the actual environment where antennas are going to operate, thus providing insight

that cannot be obtained from lab measurements, which are typically focused on ideal, free-space scenarios. Their other advantages include access to appropriate measurement locations, high-resolution of the measured position, the use of simple hardware, reduced ground-reflection effects, and the potential to extract additional parameters.

AIRBORNE ANTENNA MEASUREMENTS

UAVs are used to measure the radiation pattern of antennas under real operating conditions, where the influence of environments, such as distortion due to a multipath or coupling to neighboring objects, can be considered. The measured radiation pattern can be utilized to detect faulty elements in an array or correct the tilt angle of an antenna and find null fills. Additionally, the measured data can be used in simulations or network planning to improve the performance of communication links. UAV-based measurement techniques have many advantages over airborne measurements with a helicopter and land-based measurements, such as a traditional drive test.

The concept of obtaining antenna measurements with a UAV is displayed in Figure 1. The UAV flies a preprogrammed path in azimuth and elevation planes around the antenna under test (AUT) and measures the radiated power at each measurement point. The power measurements can be performed using either a power sensor or a software-defined radio, which also acts as a spectrum analyzer. Alternatively, the UAV can be equipped with a transmitter so that the AUT becomes the receiver [21], [22]. We briefly discuss these passive and active measurement methods in more detail. The advantages of using UAVs for antenna measurements are summarized in Table 1 and are discussed in the next section.

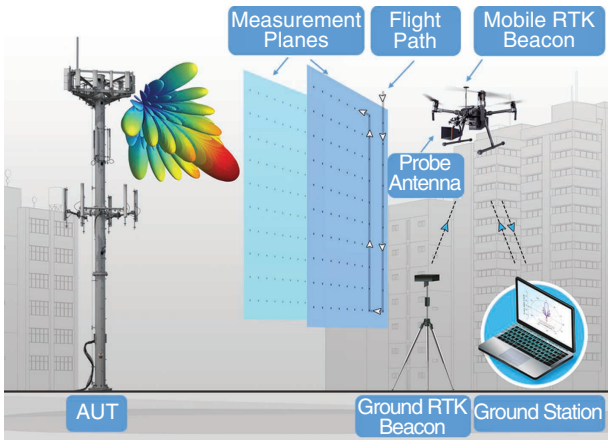

FIGURE 1. Antenna measurements obtained using UAVs. The UAV performs the measurements at preprogrammed waypoints. A real-time kinematic (RTK) system is used for high-precision positioning. The ground station establishes the communication link between the UAV and the control software. This setup has been used in [17] and [18] for antenna measurements. AUT: antenna under test.

TIME, EXPENSES, ENVIRONMENTAL EFFECTS, AND SAFETY OF PERSONNEL

In measurements with UAVs, no heavy and expensive equipment, like the kinds used in drive tests, is needed, and the results are collected much faster. In addition, UAVs rely on green technology because they are powered by batteries and create no pollution. Another benefit of using UAVs is to improve the safety of personnel. In fact, cellular antennas are mounted on towers that are typically 30 m to 60 m in height. UAVs can access these wireless transmitters easily, whereas human climbers cannot safely reach them. Moreover, UAVs can work around towers more safely and faster and provide more information than manual, land-based inspections. This makes it permissible for mobile operators to quickly address problematic areas to improve the performance of the network, which enhances the overall customer experience and satisfaction with operators' services.

ACCESS TO APPROPRIATE MEASUREMENT POINTS

Compared to land-based measurements, access to appropriate measurement points is much easier with UAVs. UAVs are

TABLE 1. A COMPARISON OF UAV-BASED MEASUREMENTS WITH THE LAND-BASED/HELICOPTER MEASUREMENT.

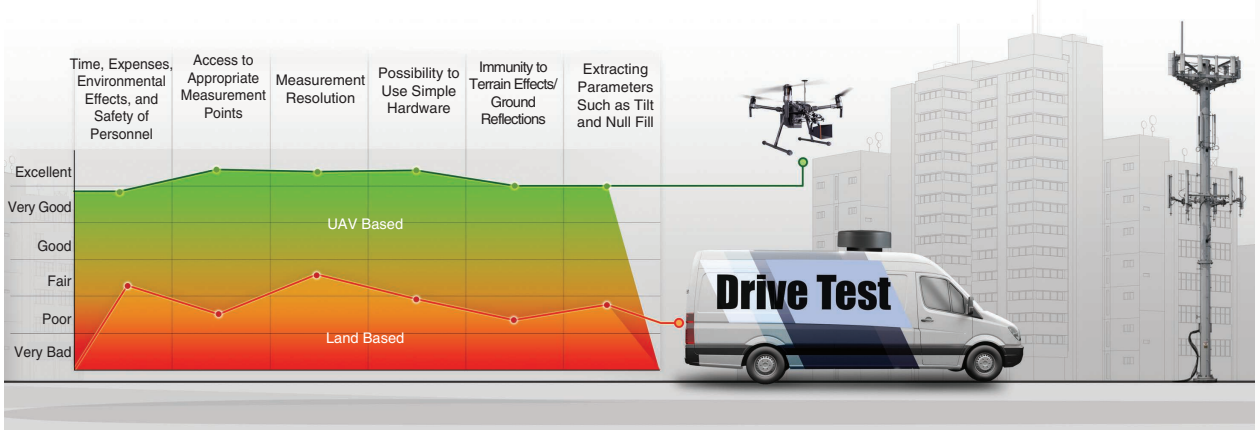

very suitable for measurements in densely populated regions where helicopters cannot fly, while land-based measurements are limited to paths accessible by car.

The array of measurement points, called *waypoints*, can form different grids, such as spherical, cylindrical, and planar. The type of measurement and the AUT [23] determine which grid is more appropriate. Using preprogrammed waypoints makes it very easy to repeat the measurements at the same points.

UAVs are very suitable for measurements in densely populated regions where helicopters cannot fly, while land-based measurements are limited to paths accessible by car.

RESOLUTION OF THE MEASURED POSITION

In practice, there is always a *positioning error*, defined as the difference between the position of each preprogrammed waypoint and the actual position of the drone. A high-precision positioning system is essential to minimizing this error. As the precision of a GPS is not sufficient for antenna measurements, a real-time kinematic (RTK) system is employed to determine the horizontal position, i.e., the latitude and longitude of the UAV with centimeter-level accuracy [21]. As discussed in the "Near-Field Measurements" section, the sampling rate for the amplitude-only near-field measurement is $\lambda/4$. The centimeter-level accuracy of approximately 1.5 cm allows for accurate measurements of antennas in the sub-6 GHz band. For the far-field measurements, the centimeter-level error is negligible because the distance between the measurement points is several meters. For a more accurate positioning, a laser tracker system with millimeter-level accuracy can be used, which enables the measurement of antennas up to 40 GHz [17]. The positioning errors can lead to a discrepancy of roughly 1 dB in the radiation pattern of the antenna [17]. A height sensor is necessary to find the vertical position of the UAV where an accurate positioning can be achieved using the laser altimeter.

The ground station monitors and controls the operations. Moreover, the measured data are sent to the ground station and analyzed by software. The Industrial, Scientific, and Medical frequency bands are used for communication with UAVs, where the telemetry link between the UAV and the ground station operates at 433 MHz and the link between the remote controller and the UAV operates at 2.4 GHz or 5.8 GHz.

SIMPLE HARDWARE

UAV-based measurements can use simple hardware, such as power detectors, because UAVs may access arbitrarily convenient positions such that the signal they measure is stronger because it is not blocked by obstacles or severely affected by multipath effects. This is not the case with measurements performed using ground vehicles, which require hardware with higher sensitivity.

REDUCED EFFECT OF GROUND REFLECTIONS

In general, when a transmitter and a receiver are in line of sight of each other, the direct wave from the transmitter, as well as the reflection from the ground, is measured by the receiver. This results in the fluctuation of the received power, which may be estimated with a two-ray model assuming a well-reflecting terrain, as qualitatively shown in Figure 2.

The effect of ground reflections can be avoided or minimized by using a UAV as presented in Figure 3. As the UAV flies relatively close to the AUT, a reflection is usually not received by the UAV antenna; or, when ground reflections are present, they are significantly attenuated by the sidelobes of the UAV antenna. Assume that we aim to measure the sidelobe level of the AUT in Figure 3. For the land-based measurement, both the direct wave from the sidelobe and the reflected wave from the main lobe are received on the ground. For the UAV-based measurement, the contribution due to the reflected wave from the main lobe is zero.

EXTRACTION OF PARAMETERS (TILT AND NULL FILL)

The tilt angle of a base station's radiation pattern can significantly affect coverage, as depicted in Figure 4. UAVs can easily measure the vertical radiation pattern of a base station antenna and therefore obtain the value of the tilt angle. Measurements of vertical patterns are hard, time consuming, and expensive using airborne measurements with a helicopter and are impossible to achieve with land-based measurements. In addition, vertical radiation-pattern measurements obtained by UAVs allow for the acquisition of further information, such as the null fills of broadcast antennas.

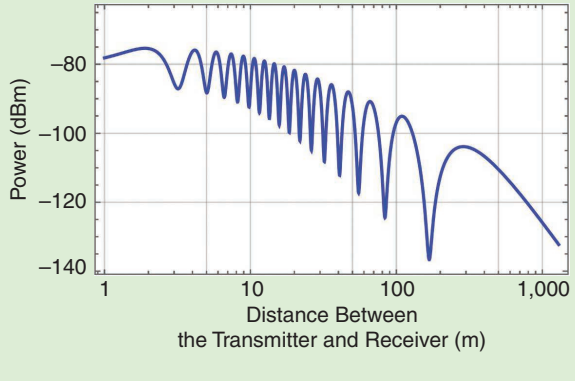

FIGURE 2. The effect of ground reflections on the received power.

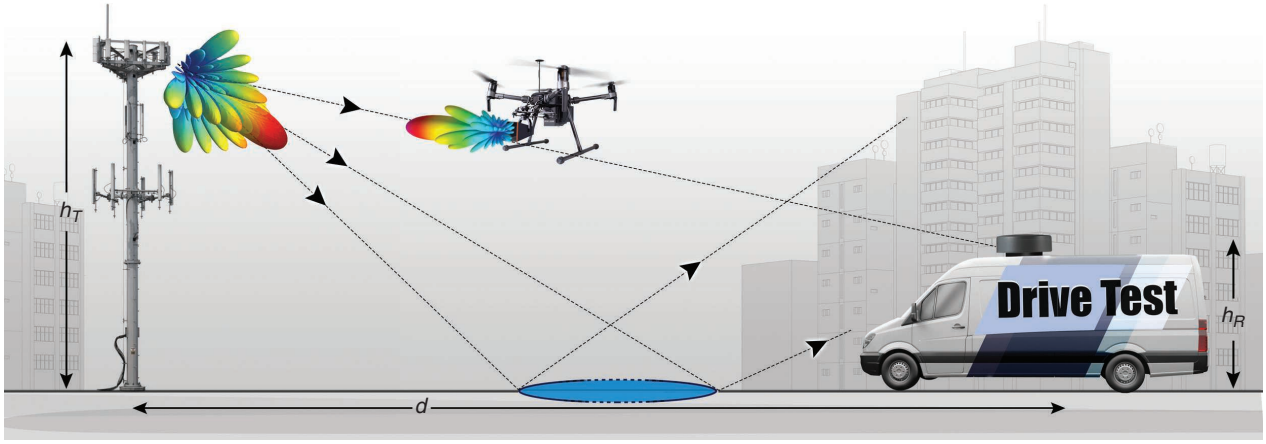

FIGURE 3. The measurements obtained from UAVs are much less sensitive to ground reflections compared to land-based measurements. In particular, the UAV in this picture does not receive ground reflections emanating from the main beam of the antenna.

FAR-FIELD MEASUREMENTS

The far field of an antenna begins from the distance $R = 2D^2/\lambda$, where D is the maximum linear dimension of the antenna and λ is the wavelength. To be well within the far field of an antenna, the distance from the antenna should be approximately 10 R because two more criteria ($R \gg D, R \gg \lambda$) must be met to be in the far field. When performing far-field measurements, one should be careful about the effects of ground reflections because the direct and reflected paths cannot always be angularly separated. In such a case, the measurements could either be corrected to account for them or avoided in favor of near-field measurements.

To obtain the vertical radiation pattern of the AUT in a plane at a specific azimuth angle, the UAV flies vertically along a straight line, as shown in Figure 5 [16]. The position of the UAV as well as the corresponding measured value for the received power is recorded. The following first two corrections (and possibly the third) must be done in the postprocessing:

1) A correction must be made to account for the actual distance between the UAV and AUT, which changes with the position of the UAV because the trajectory is not on a spherical surface centered at the AUT.
2) A correction must be made to account for the orientation of the probe antenna, especially when the antenna mounted on the UAV is directive, such as the one discussed in [16]. The orientation affects the gain because at some locations, the probe antenna may receive the signal from the sidelobe, while it may receive one from the main lobe at the other locations [22].
3) A correction due to the ground-reflection effect may also be necessary if the UAV flies far from the AUT.

The measurements of vertical antenna patterns are helpful to determine the optimal flying height for subsequent horizontal pattern measurements. This height is most often the height at which the vertical radiation pattern is at its maximum. Moreover, the effect of UAV orientation must be considered [22] as the UAV can have a slight tilt due to limited accuracy of the navigation system as well as external disturbances such as wind. After the vertical flight, which determines the optimal height for horizontal pattern measurements, the UAV flies at that height on a circular path to measure the horizontal radiation pattern of the AUT, as shown in Figure 6.

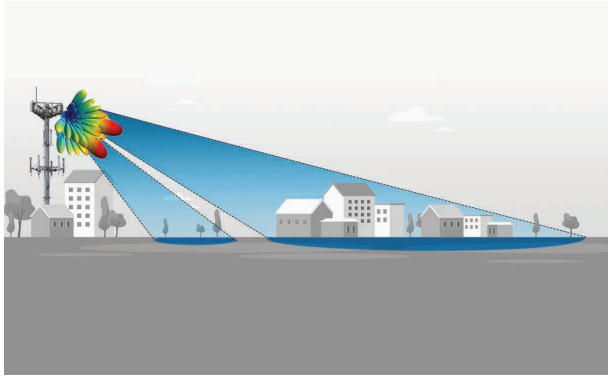

FIGURE 4. A qualitative description of the effect of antenna tilt on the coverage. A tilted antenna shifts the covered area, which results in a lack of coverage for a large number of users. Note that the figure is not drawn to scale.

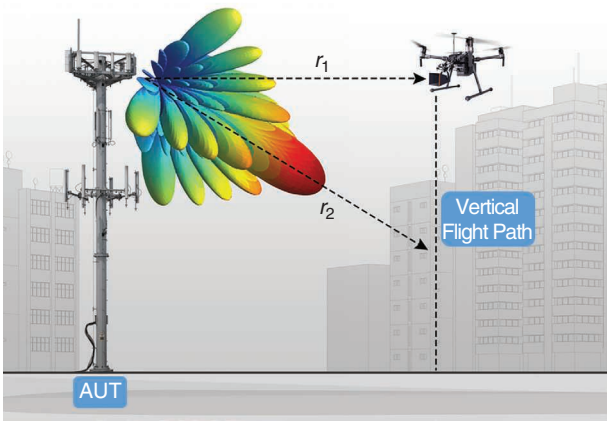

FIGURE 5. A vertical flight used to obtain the vertical radiation pattern.

The passive measurements can also be used for the in situ calibration of radars, where the conventional method is to use passive or active targets with a known radar cross section (RCS). These targets are mounted on special supporting structures and cannot be easily moved along a desired direction, which limits the complete testability of the radar's test range [24]. Moreover, the supporting structure itself affects the measurement results, and, most importantly, it is vulnerable to ground reflections if the height of the target is not large enough [24]. These problems can be solved using airborne targets, where balloons or aircrafts are utilized; however, these are expensive, not flexible enough for all kinds of tests, and cannot be easily operated. UAVs are cost-effective, can access the appropriate measurement points easily, are much less vulnerable to ground reflections, and are flexible in terms of operation and scan strategy. Hence, UAVs can be used for radar calibrations with a mounted target with a known RCS, such as a corner reflector [24]–[27].

The UAV can also carry a transmitter and act as a far-field source where the UAV flies at a constant height above the AUT [28]–[30]. Different scan strategies, such as Cartesian, radial, and azimuthal 3D rasters, have been used to investigate flight efficiency in terms of the covered area versus time [31]. Choosing the appropriate scan strategy will minimize the flight duration. Other parameters, such as sampling density, path loss, and flight accuracy, should be considered when choosing a certain scan strategy.

This active measurement solution is appropriate to characterize reflectors, arrays, and very high/ultrahigh frequency antennas under real operating conditions. This technique has been used to measure the performance of low-frequency arrays (LOFARs) used in radio astronomy, which operate at two frequency bands: from 10 MHz to 90 MHz or from 120 MHz to 240 MHz [32], [33]. For example, in [31], the intrinsic cross-polarization parameter is measured to assess the polarimetric performance of the LOFAR. Another example is evaluating the effect of mutual coupling on the radiation pattern of elements for the LOFAR stations [33].

NEAR-FIELD MEASUREMENTS

Near-field measurements are performed to avoid the challenges associated with far-field measurements; however, near-field measurements require more complicated postprocessing. The challenges of far-field measurements become more evident for large antennas, which have a larger far-field distance; at larger distances, the measurements are more vulnerable to ground reflections. In addition, several flights may be necessary for full pattern measurements because the flight path becomes much longer at large distances from the antenna. Another challenge associated with far-field measurements is that they may require flight over restricted areas, such as crowds of people, airports, or military bases, where the flight is either prohibited or needs special permission from appropriate authorities. However, measurements at larger distances from the AUT have the advantage of being less sensitive to positioning errors, as the measurement points can have large separations.

For near-field measurements, an amplitude-only measurement technique using a simple power sensor, which eliminates the need for a coherent receiver to measure the phase, has been developed [17], [34]–[36]. The phase information can be retrieved by performing measurements at two or more measurement planes, as displayed in Figure 1. For amplitude-only measurements, the distances between the two neighboring measurement points on each plane must be smaller than $\lambda/4$, which is twice the Nyquist rate. In the case of amplitude and phase measurements, the sampling rate becomes $\lambda/2$ [35]. In the next step, the measurement data are used to find the equivalent current distribution on the antenna aperture where these equivalent currents radiate the same field as the AUT outside the reconstruction domain (the second-equivalence principle). These currents are then used to transform the near-field information to far-field radiation pattern; this is called the *phaseless source reconstruction method*; compared to other methods such as indirect holographic techniques [17], it is very simple and inexpensive in terms of hardware. Figure 7 presents the current distribution on the apertures of an array of horn antennas using near-field measurements.

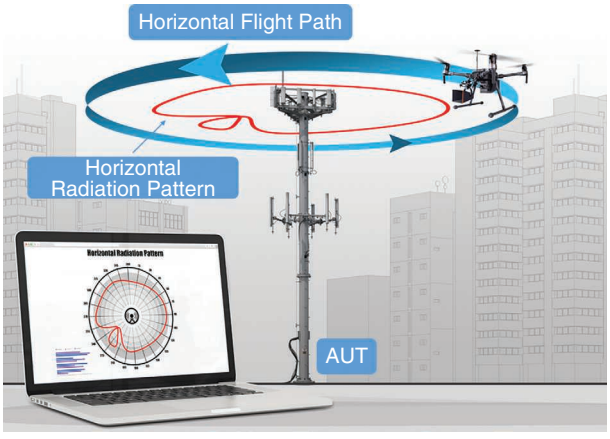

FIGURE 6. A circular flight used to obtain the horizontal radiation pattern.

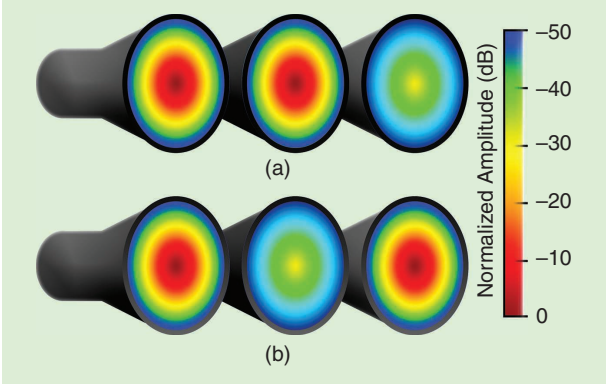

FIGURE 7. An array of circular horn antennas with reconstructed currents at the aperture of the antenna. (a) Faulty element on the right and (b) faulty element in the middle: The current distribution of the two faulty elements can, e.g., be related to the problems in the feed of the antenna.

Choosing the appropriate probe antenna for near-field measurements is very important. One should avoid using highly directive antennas because orientation misalignments between the AUT and the probe, due to UAV attitude uncertainties, are more prominent compared to an antenna with low directivity. In addition, probe correction needs to be done when using highly directive antennas; therefore, using low-gain antennas, such as microstrip antennas, is more appropriate for near-field measurements.

UAV PROBE ANTENNAS

Parameters such as weight, size, bandwidth, and polarization purity are also important when choosing a probe antenna for near- and far-field measurements. The antennas typically utilized for high-frequency measurements with UAVs are 1) dipoles used for measurements when the transmitter is mounted on the UAV; 2) directional antennas such as 3D-printed, corrugated horn antennas used for the measurement of satellite communication systems; and 3) other directional antennas, such as Yagi and log periodic, used for direction finding.

DIRECTION FINDING AND INTERFERENCE HUNTING

Direction-finding systems are employed to determine the direction of incoming electromagnetic waves. This technique is used in satellite communications and radar systems and for locating the source of interference, which is called *interference hunting* [37], [38]. UAVs help to greatly simplify direction-finding and interference-hunting procedures and thus save time and money.

Having a clean spectrum is essential for mobile networks because the interference decreases the network capacity. There is not a simple relationship between the network capacity and interference, but an approximate criterion is that for a 10 dB decrease in signal-to-interference-plus-noise ratio, 50% of the network capacity is lost [39]. Some of the more familiar effects of interference are poor voice quality, connection failures, and low throughput.

The interference can be categorized into two general types: in- and out-of-band interference. In-band interference is caused by an overlap in operating bandwidth of the transmitter and the receiver. The out-of-band interference is caused by filtering imperfections in the transmitter and the receiver, which operate at different frequencies but are located close to each other. In this article, we focus on in-band interference because out-of-band interference is more a design issue.

The sources of in-band interference are very different in nature and can be categorized in terms of duration (intermittent versus perpetual), bandwidth (narrow versus wideband), type of source (intentional versus nonintentional), and generating frequencies (harmonics and intermodulation). How severely the interference affects a communication link depends strongly on the environment and characteristics of the communication link.

The first step in interference hunting is to collect as much information about the interfering signal as possible because this information facilitates the identification of the source of interference. This can be done, for example, by analyzing the spectrum of the received signal or sometimes demodulating the signal at the receiver. In the next step, an omnidirectional antenna, together with a map and software, is used to scan an area, which enables the verification of the presence of the source of interference and its approximate location. This phase is called *drive around* for land-based measurements. After this, the exact location of the interferer is found using a directional antenna, such as Yagi or log periodic. This phase is called *walk around* in land-based measurements.

A Yagi antenna is more directional than a log periodic; however, its bandwidth of roughly 1 GHz is not large enough compared to a log-periodic antenna with a bandwidth from 300 MHz to 7 GHz. A bandpass filter is also needed to filter the signals outside the range of interest for interference hunting. This is specially recommended for regions with high signal strength. Combining this with a real-time spectrum analyzer (RSA) can further accelerate the process because transients and cochannel interference signals can be detected relatively easily using an RSA.

Here we focus on interference in mobile networks and show how UAVs are useful for interference hunting. Electronic devices, illegal or faulty transmitters, harmonics, and the passive intermodulation caused, e.g., by the rusty bolt-effect, can potentially create interference in mobile networks. Finding the source of interference can sometimes be extremely cumbersome and time consuming. This is where UAVs can become helpful and facilitate the process of interference hunting, as we see in the following examples.

The first example is about cochannel interference, which occurs because LTE networks typically communicate on the same channel; thus, the interference could happen due to sector-overlap issues. It is known that the number of detected cells increases as the height increases [19]; therefore, using a UAV could increase the chance of finding interferers.

Another scenario occurs when the source of interference is located on the roof of a building or inside an apartment in a large building, both of which are difficult to access [19]. Propagation effects such as attenuation, reflection, and multipath make interference hunting more complicated. Getting away from the ground helps minimize these propagation effects, and this is exactly why interference hunters go to the roof of a building. Doing so, however, requires permission, which can take a long time and may not always be possible. This is where drones become extremely helpful as they can easily reach high altitudes, thus eliminating the need to access roofs.

Attenuation may be helpful when it weakens the interference signal. In such a case, however, attenuation is not helpful for interference hunting because the received signal on the ground can become extremely weak and difficult to detect, while the base station antenna installed at a large height can easily receive the interference signal. Using drones can significantly accelerate the process of interference hunting by flying to a location with a better reception from the interferer.

An example of the effect of reflections is shown in Figure 8, which emphasizes that the observers on the ground

receive the interfering signal along a direction that does not point to the location of the source of interference, due to the reflections. Therefore, it is advisable for land-based interference hunting to maintain an adequate distance from the reflecting objects. Again, in this case, using a drone can facilitate the process of interference hunting, as drones are much less prone to reflections due to their large distance from the objects on the ground. Multipath effects are similar to reflections, the exception being that the signals seemingly come from many different places due to multiple reflections.

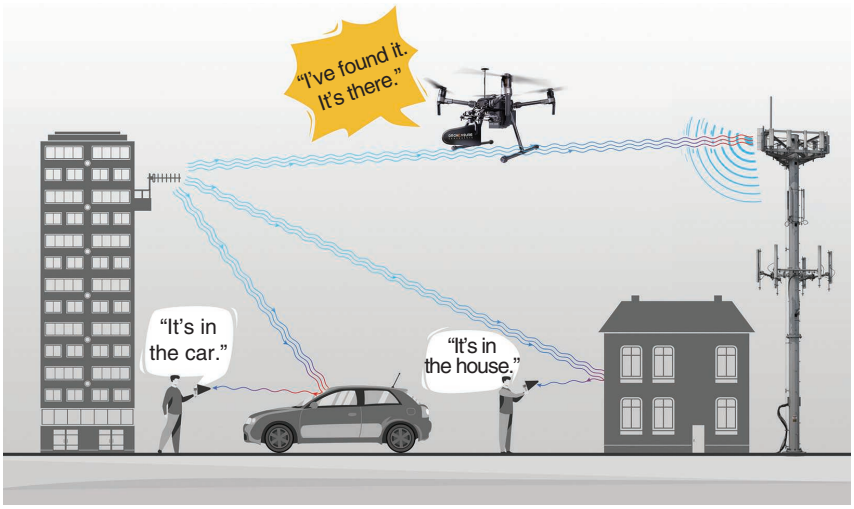

FIGURE 8. An illustration of interference hunting assuming that the interference source is the antenna on the balcony, which radiates toward the tower, the UAV, the shorter building, and the car. The energy radiated to the car is reflected toward the observer on the left and the energy radiated toward the shorter building is reflected to the observer on the right. The interfering signal appears to come from the car for the observer to the left or from the shorter building to the observer on the right. However, the UAV is much less prone to reflections and can easily locate the interference using its directional log-periodic antenna.

MOBILE NETWORK TESTING

HF measurements and optimizations are necessary to improve the performance of current mobile networks as well as the incoming 5G technology and future networks. 5G mobile communications promote the development of innovative services and applications such as Industry 4.0, autonomous driving, the Internet of Things (IoT), and UAV services [40], [41]. As the quality of the link in 5G networks is critical for some applications, such as autonomous driving, it is of the highest importance to make sure that the communication links perform as expected. In this section, we discuss how UAVs can be used to measure LTE parameters and how the UAVs themselves are affected when they use LTE services.

The quality of service of mobile networks must be monitored regularly. One method utilized to do so is crowd sensing, which collects data using a huge number of sensors and analyzes these data to extract the various parameters of mobile communication networks. The most important parameters of the mobile networks are briefly discussed next.

Each cell in an LTE network continuously sends a cell-specific reference signal (RS). The power received by the user equipment (UE), which can be a cell phone, vehicle, or any other device, is called RS received power (RSRP). The typical values for RSRP lie between –140 dB and –50 dBm, where –50 dBm equates to an excellent reception. As the received power decreases, the reception becomes worse and the data speed reduces. Usually, below –110 dBm, the connection becomes very bad, and below –125 dBm there is likely no reception. The received signal strength indicator (RSSI) shows the sum of all the received powers, consisting of noise and the useful signal.

RS received quality (RSRQ), another parameter that measures reception quality, entails the effect of noise and is proportional to the ratio of the RSRP to the RSSI; so RSRQ is somehow similar to the signal-to-noise ratio, i.e., the higher the RSRQ value, the better the reception quality. This means that if the RSRP is large but the RSRQ is low, there will be no good reception despite the large RSRP. The typical values of RSRQ lie between –20 dB and –3 dB. The values below –15 dB signify a very bad reception quality.

UAVs can be used to measure mobile network parameters for serving and neighboring cells. Some of these parameters are RSRP, RSRQ, RSSI, radio-link failure, throughput, latency, the number of detected cells, the distance to serving and neighboring cells, and physical cell identity allocation changes. These data can be used for the characterization and optimization of mobile networks. Most importantly, these data are necessary to assess network performance in the event that a network provides services for UAVs, such as delivery drones. Note that the UAVs are served by the sidelobes of the cell's antennas, as depicted in Figure 9. Determining the quality of the link is essential for many drone services; therefore, the best way to verify the quality of a mobile network for drone services is to use UAVs themselves to test it.

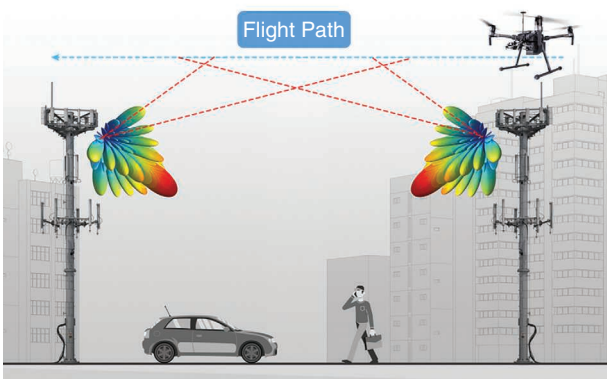

FIGURE 9. For some services, such as deliveries, UAVs fly above the base stations. The communication link is maintained by sidelobes.

Another important technology for industry as well as consumer applications is the IoT. The optimal placement of base stations is essential for interference-free IoT mesh [42], where UAV-based measurements of the mobile network parameters, such as the RSSI, can be used for the optimal deployment of base stations.

RF IMAGING

RF imaging has important advantages compared to optical imaging, the most important of which are no dependence on daylight and significantly less dependence on the weather so that an area of interest can be monitored independent of cloud-cover conditions and lighting. RF imaging techniques have been used to image buried objects, such as land mines or underground tunnels [43], [44].

For optical imaging, the light reflected from an object enters a camera or telescope. RF imaging works in a similar way by gathering electromagnetic waves scattered from the objects where the source of the scattered waves is an RF source, which is akin to the operation of a radar.

The resolution of an image using optical imaging depends on the wavelength and size of the aperture that collects the reflected waves. Smaller wavelengths result in higher resolution. These criteria also apply to RF imaging, i.e., smaller RF wavelengths result in higher resolution, and the size of the antenna's aperture determines the resolution of the images. This means that for high-resolution images, antennas with large apertures are needed.

Employing UAVs not only accelerates the surveillance and imaging of an area; it also allows for higher resolutions using SAR algorithms.

A technique known as *synthetic aperture radar* (*SAR*) [45] allows for the acquisition of high-resolution images with small antennas by enlarging the size of the antenna aperture synthetically. With this technique, the antenna is moved over the area of interest to collect waves scattered from different directions, which mimics a large aperture. UAVs are perfect for SAR imaging, where a monostatic radar module with relatively small antennas, such as log-periodic or helical, can be installed on the UAV to gather the scattered waves [46]–[50].

Then, SAR algorithms such as delay and sum and phase-shift migration can be used to analyze the collected data. The concept of RF imaging with a UAV is presented in Figure 10. Accurate positioning using an RTK system is also necessary for RF imaging with a UAV. Employing UAVs not only accelerates the surveillance and imaging of an area; it also allows for higher resolutions using SAR algorithms.

The same concept of imaging using radars can be utilized for subsurface imaging. This technique uses ground-penetrating radar (GPR) where electromagnetic waves penetrate the surface and are scattered by a buried object. UAVs can also use GPR for the underground inspection of pipes, landmines [44], [51], and archaeological sites [52]. The main advantages of UAVs here are that large areas can be scanned relatively fast and that combining GPR with SAR enables high-resolution GPR images.

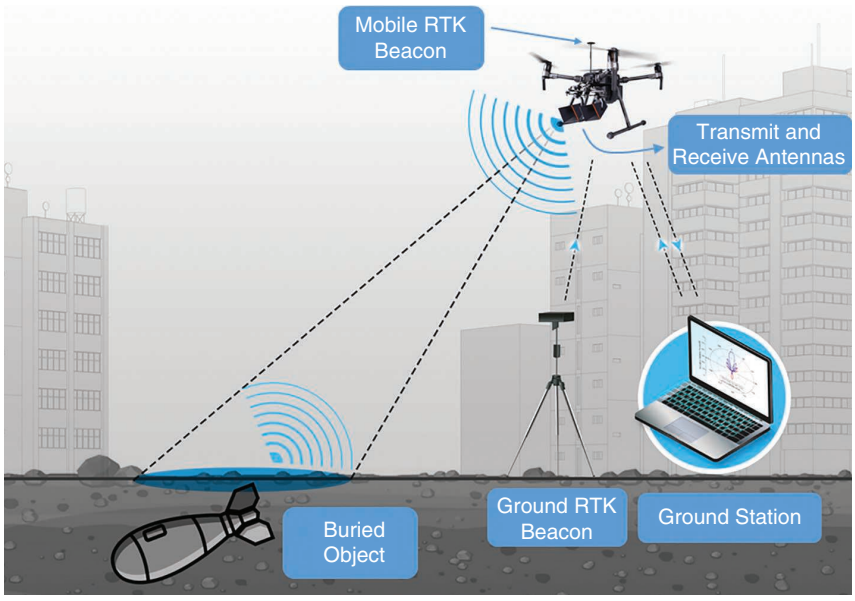

FIGURE 10. The same setup as in Figure 1 as well as a radar module and two antennas, which can be used for RF imaging, such as to identify buried objects.

STRUCTURE OF A UAV

In this section, we briefly discuss how a UAV flies and how it can be controlled using the example of a quadcopter. A quadcopter has four motors, and opposite motors have the same direction of rotation, whereas the adjacent motors have a different direction of rotation, as shown in Figure 11. This helps balance the torques exerted upon the body of the quadcopter. The spinning propellers push the air downward, creating a thrust force that keeps the UAV aloft.

It is known from mechanics that the motion of a rigid body can be expressed as a combination of a translational motion (x, y, z) and a rotational motion (φ, θ, ψ) around the roll, pitch, and yaw axes. This also applies to a UAV, as depicted in Figure 11 [53]. The Newton and Euler equations are

used to describe the translational and rotational motions of the UAV, respectively. These equations result in a set of coupled partial differential equations, where analytical solutions can be obtained using small-angle approximations.

Each motor contributes to three motions, namely, hovering and the rotations around two axes. For example, motor 1 in Figure 12 is responsible for rotations around the y- and z-axes. As the UAV takes off vertically in hovering mode, all of the motors have the same speed. To generate motion around a certain axis, the speed of the motors should change (see Figure 12).

NAVIGATION SYSTEM

The motion of a UAV is a combination of translational and rotational motions. The information corresponding to these two motions can be obtained by using the appropriate sensors, as shown in Figure 13. The GPS and the barometer (pressure sensor) provide the position of the UAV. The GPS provides the latitudinal and longitudinal information corresponding to (x,y), and the barometer gives the height information matching z. Note that the GPS system may be vulnerable to a loss of signal due to a variety of reasons, such as a lack of satellite visibility and jamming or spoofing.

The inertial measurement unit (IMU) sensor, which consists of a gyroscope and an accelerometer, delivers the angular or attitude information corresponding to the orientation of the UAV. More specifically, the three-axis gyroscope delivers the angular velocity, and the three-axis accelerometer delivers the acceleration, which helps to find Euler's angles. The IMUs are based on microelectromechanical system technology—inexpensive, light, and small components with low power consumption.

A magnetometer sensor (compass), which provides data on the yaw angle regardless of UAV orientation, can also be used; this helps to find the heading of the UAV. The combination of an IMU and magnetometer is called the *attitude and heading reference system*.

Now assume that the UAV with a known current position at point A wants to fly to a desired final position at point B. The navigation system serves two main purposes when the UAV flies from A to B. First, it ensures that the quadcopter is stable in all of its rotational axes, i.e., it automatically levels the quadcopter. Second, it tries to minimize the difference between the current position of the UAV and its final desired position.

Different algorithms, such as the Kalman filter, are used to fuse the information provided by the sensors and make decisions to control the UAV. Also, the traditional proportional-derivative and proportional-integral-derivative controllers work very well for many UAV applications.

The position of a UAV can be determined by either a remote controller (joystick) or a predefined path. For automatic measurements (e.g., antenna), an autonomous UAV should be used because it can be preprogrammed to follow a predefined path, which makes the measurement process very easy.

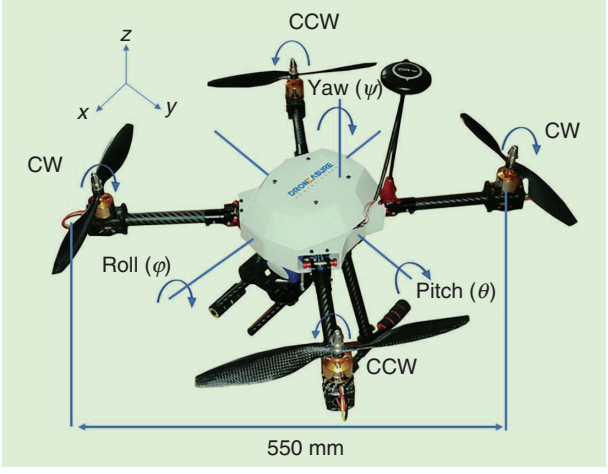

FIGURE 11. A representation of the roll, pitch, and yaw axes as well as the directions of motor rotation in a quadcopter. φ is the rotation around the x-axis, θ is rotation around the y-axis, and ψ is the rotation around the z-axis. CW: clockwise; CCW: counter-clockwise.

LIMITATIONS

The limitations for using UAVs can be classified into two groups: regulatory and physical. Some examples of regulatory limitations are the maximum flight level (120 m in the European Union), weight (a 2.4 kg maximum payload for quadcopters), UAV licenses and other considerations, and operation beyond the visual line of sight, which is only allowed with special permission from the appropriate authority. These regulations are continuously updated to make them compatible with the needs of industry and for personal use. The physical limitations consist of flight time, operation in different types of weather, and the size of the UAV. The flight time is within 20 to 30 min depending on the weight of the UAV, its speed, and other related factors. Tethered UAVs can also be used if much longer flight times are necessary, such as in the case of lengthy

Force/Moment	ω_1	ω_2	ω_3	ω_4
Roll Moment	+		−	
Pitch Moment		−		+
Yaw Moment	+	−	+	−
Vertical Thrust	+	+	+	+

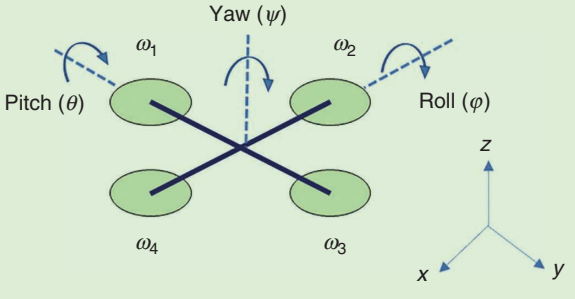

FIGURE 12. The variations of motor speeds and the corresponding changes in the yaw, pitch, and roll angles.

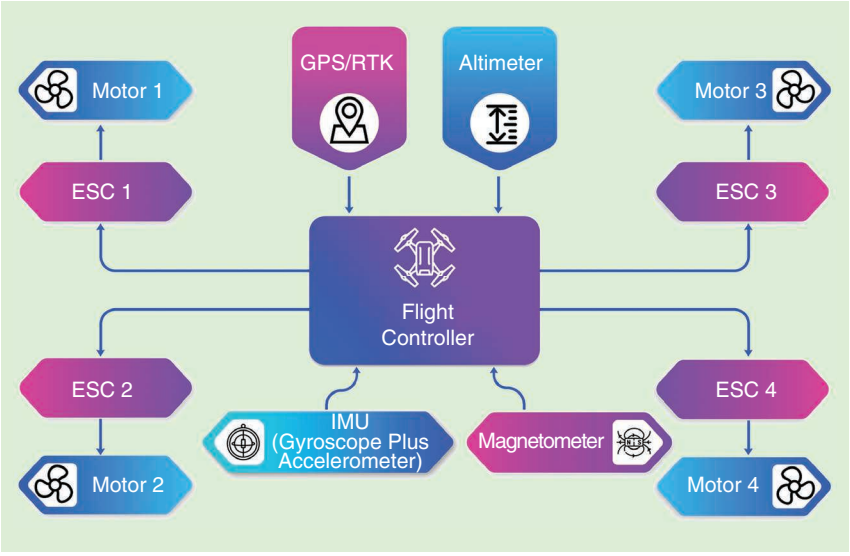

FIGURE 13. A block diagram of the UAV navigation system. ESC: electronic speed controller.

interference-hunting operations. The largest size of a quadcopter is approximately 450 mm to 550 mm.

CONCLUSIONS

In this article, we reviewed the cutting-edge technology of HF measurements with UAVs. Using UAVs for measurements has several advantages compared to conventional land-based measurements and helicopters. The major benefits for commercial wireless communications are improved accuracy, reduced cost, higher speeds, and the potential to perform measurements in the actual environment where base station antennas operate, thus allowing for various types of diagnostics and the extraction of information that cannot be obtained from laboratory measurements. HF measurements may be used for radar-imaging applications, and it is possible that future applications will include more complex measurements that require the use of flocks of drones. Other HF measurements that may benefit from UAVs are antenna measurements for applications different from cellular communications, such as antenna-pattern measurements for oceanographic radars [54], the detection of disaster victims [55], and specific absorption-ratio measurements for health concerns.

ACKNOWLEDGMENTS

This article was partially supported by RWTH Aachen University, EXIST-Gründerstipendium, and the University of Illinois at Chicago. The opinions, findings, and conclusions or recommendations expressed in this article are those of the authors and do not necessarily reflect the views of RWTH Aachen University, EXIST Gründerstipendium, or the University of Illinois at Chicago.

AUTHOR INFORMATION

Alan Salari (alan.salari22@gmail.com) is affiliated with the Andrew Electromagnetics Laboratory, the University of Illinois at Chicago, Chicago, Illinois, 60607, USA. He is the founder of Droneasure. He is a microwave engineer and physicist with experience in satellite communications and superconducting quantum computing systems. He is a Member of IEEE.

Danilo Erricolo (derric1@uic.edu) is a professor and the director of graduate studies in the Department of Electrical and Computer Engineering; the director of the Andrew Electromagnetics Laboratory; and an adjunct professor of bioengineering, all at the University of Illinois at Chicago, Chicago, Illinois, 60607, USA. His research interests include wireless communications, antenna design, electromagnetic propagation and scattering, and magnetic resonance imaging. He is a Fellow of IEEE.

REFERENCES

[1] Y. Inoue and M. Yokoyama, "Drone-based optical, thermal, and 3D sensing for diagnostic information in smart farming—Systems and algorithms," in *Proc. 2019 IEEE Int. Geosci. Remote Sens. Symp. (IGARSS 2019)*, Yokohama, Japan, pp. 7266–7269. doi: 10.1109/IGARSS.2019.8898736.

[2] M. Bacco et al., "Smart farming: Opportunities, challenges and technology enablers," in *Proc. 2018 IoT Vertical Topical Summit Agriculture - Tuscany (IOT Tuscany)*, Tuscany, pp. 1–6. doi: 10.1109/IOT-TUSCANY.2018.8373043.

[3] S. V. Sibanyoni, D. T. Ramotsoela, B. J. Silva, and G. P. Hancke, "A 2-D acoustic source localization system for drones in search and rescue missions," *IEEE Sensors J.*, vol. 19, no. 1, pp. 332–341, Jan.1, 2019. doi: 10.1109/JSEN.2018.2875864.

[4] N. Kumar, D. Puthal, T. Theocharides, and S. P. Mohanty, "Unmanned aerial vehicles in consumer applications: New applications in current and future smart environments," *IEEE Consum. Electron. Mag.*, vol. 8, no. 3, pp. 66–67, May 2019. doi: 10.1109/MCE.2019.2892278.

[5] A. Claesson et al., "Drones may be used to save lives in out of hospital cardiac arrest due to drowning," *Resuscitation*, vol. 114, pp. 152–156, May 2017. doi: 10.1016/j.resuscitation.2017.01.003.

[6] C. A. Thiels, J. M. Aho, S. P. Zietlow, and D. H. Jenkins, "Use of unmanned aerial vehicles for medical product transport," *Air Med. J.*, vol. 34, no. 2, pp. 104–108, 2015. doi: 10.1016/j.amj.2014.10.011.

[7] L. Tang and G. Shao, "Drone remote sensing for forestry research and practices," *J. Forestry Res.*, vol. 26, no. 4, pp. 791–797, Dec. 2015. doi: 10.1007/s11676-015-0088-y.

[8] E. Natalizio, R. Surace, V. Loscri, F. Guerriero, and T. Melodia, "Filming sport events with mobile camera drones: Mathematical modeling and algorithms," HAL, Lyon, France, Res. Rep. hal-00801126, 2012.

[9] S. Daftry, C. Hoppe, and H. Bischof, "Building with drones: Accurate 3D facade reconstruction using MAVs," in *Proc. IEEE Int. Conf. Robot. Automat. (ICRA)*, May 2015, pp. 3487–3494. doi: 10.1109/ICRA.2015.7139681.

[10] S. W. Loke, M. Alwateer, and V. S. A. A. A. Don, "Virtual space boxes and drone-as-reference-station localisation for drone services: An approach based on signal strengths," in *Proc. 2nd Workshop Micro Aerial Vehicle Netw., Syst., Appl. Civilian Use*, 2016, pp. 45–48. doi: 10.1145/2935620.2935627.

[11] A. Shukla, H. Xiaoqian, and H. Karki, "Autonomous tracking and navigation controller for an unmanned aerial vehicle based on visual data for inspection of oil and gas pipelines," in *Proc. 16th Int. Conf. Control, Autom. Syst. (ICCAS)*, Oct. 2016, pp. 194–200. doi: 10.1109/ICCAS.2016.7832320.

[12] A. Majd, A. Ashraf, E. Troubitsyna and M. Daneshtalab, "Using optimization, learning, and drone reflexes to maximize safety of swarms of drones," in *Proc. 2018 IEEE Congr. Evol. Comput. (CEC)*, Rio de Janeiro, pp. 1–8. doi: 10.1109/CEC.2018.8477920.

[13] C. Seiber, D. Nowlin, B. Landowski and M. E. Tolentino, "Tracking hazardous aerial plumes using IoT-enabled drone swarms," in *Proc. 2018 IEEE 4th World Forum Internet of Things (WF-IoT)*, Singapore, pp. 377–382. doi: 10.1109/WF-IoT.2018.8355118.

[14] "2018 commercial drone industry trends report." DroneDeploy.com. https://www.dronedeploy.com/resources/ebooks/2018-commercial-drone-industry-trends-report/ (accessed Nov. 1, 2020).
[15] "The drone market report 2019-2024." Droneii.com. https://droneii.com/product/drone-market-report (accessed Nov. 1, 2020).
[16] J. M. Miller and E. Decrossas, "Using small unmanned aerial systems and helium aerostats for far-field radiation pattern measurements of high-frequency antennas," in *Proc. 2018 IEEE Conf. Antenna Measurements Appl. (CAMA)*, Vasteras, pp. 1–4. doi: 10.1109/CAMA.2018.8530671.
[17] M. García-Fernández et al., "Antenna diagnostics and characterization using unmanned aerial vehicles," *IEEE Access*, vol. 5, pp. 23,563–23,575, Sept. 2017. doi: 10.1109/ACCESS.2017.2754985.
[18] Y. A. Lopez et al., "Airborne systems and method for the characterisation and measurement of radiating systems or antennas" U.S. Patent 16/490 714, 2020.
[19] R. Amorim, H. Nguyen, J. Wigard, I. Z. Kovács, T. B. Sorensen, and P. Mogensen, "LTE radio measurements above urban rooftops for aerial communications," in *Proc. 2018 IEEE Wireless Commun. Netw. Conf. (WCNC)*, Barcelona, pp. 1–6. doi: 10.1109/WCNC.2018.8377373.
[20] M. Garcia-Fernandez, Y. Alvarez-Lopez, B. Gonzalez-Valdes, Y. Rodriguez-Vaqueiro, A. Arboleya-Arboleya, and F. L. Heras, "Recent advances in high-resolution ground penetrating radar on board an unmanned aerial vehicle," in *Proc. 2019 13th Eur. Conf. Antennas Propagation (EuCAP)*, Krakow, Poland, 2019, pp. 1–5.
[21] F. Paonessa et al., "Characterization of the Murchison Widefield array dipole with a UAV-mounted test source," in *Proc. 2019 13th Eur. Conf. Antennas Propagation (EuCAP)*, Krakow, Poland, pp. 1–4.
[22] F. Paonessa et al., "Effect of the UAV orientation in antenna pattern measurements," in *Proc. 2015 9th Eur. Conf. Antennas Propagation (EuCAP)*, Lisbon, pp. 1–2.
[23] M. Garcia-Fernandez, Y. Alvarez-Lopez, and F. L. Heras, "Evaluation of an unmanned aerial system for antenna diagnostics and characterization," in *Proc. 12th Eur. Conf. Antennas Propagation (EuCAP 2018)*, London, U.K., 2018, pp. 1–5. doi: 10.1049/cp.2018.0899.
[24] F. Paonessa et al., "UAV-mounted corner reflector for in-situ radar verification and calibration," in *Proc. 2018 IEEE Conf. Antenna Measurements Appl. (CAMA)*, Vasteras, pp. 1–4. doi: 10.1109/CAMA.2018.8530616.
[25] A. J. Knisely and P. J. Collins, "Utilization of an octocopter as a two-way field probe for electro-magnetic field measurements at an outdoor radar cross section range," in *Proc. AMTA*, Austin, TX, Nov. 2016, pp. 1–6.
[26] S. Duthoit et al., "A new approach for in-situ antenna characterization, radome inspection and radar calibration, using an unmanned aircraft system (UAS)," *IEEE Radar Conf.*, Seattle, WA, June 2017, pp. 669–674.
[27] J.-S. Suh, L. Minz, D.-H. Jung, H.-S. Kang, J.-W. Ham, and S.-O. Park, "Drone-based external calibration of a fully synchronized Ku-band heterodyne FMCW radar," *IEEE Trans. Instrum. Meas.*, vol. 66, no. 8, pp. 2189–2197, Aug. 2017. doi: 10.1109/TIM.2017.2687518.
[28] G. Pupillo et al., "Medicina array demonstrator: Calibration and radiation pattern characterization using a UAV-mounted radio-frequency source," *Exp. Astron.*, vol. 39, no. 2, pp. 405–421, 2015., doi: 10.1007/s10686-015-9456-z.
[29] G. Virone et al., "Antenna pattern measurement with UAVs: Modeling of the test source," in *Proc. 2016 10th Eur. Conf. Antennas Propagation (EuCAP)*, Davos, pp. 1–3. doi: 10.1109/EuCAP.2016.7481744.
[30] F. Paonessa, G. Virone, P. Bolli, G. Addamo, S. Matteoli, and O. A. Peverini, "UAV-based antenna measurements: Improvement of the test source frequency behavior," in *Proc. 2018 IEEE Conf. Antenna Measurements Appl. (CAMA)*, Vasteras, pp. 1–3. doi: 10.1109/CAMA.2018.8530506.
[31] F. Paonessa, G. Virone, P. Bolli, and A. M. Lingua, "UAV-based antenna measurements: Scan strategies," in *Proc. 2017 11th Eur. Conf. Antennas Propagation (EUCAP)*, Paris, pp. 1303–1305. doi: 10.23919/EuCAP.2017.7928721.
[32] F. Paonessa et al., "In-situ verification of aperture-array polarimetric performance by means of a micro UAV: Preliminary results on the LOFAR low band antenna," in *Proc. 2018 2nd URSI Atlantic Radio Science Meeting (AT-RASC)*, Meloneras, pp. 1–4. doi: 10.23919/URSI-AT-RASC.2018.8471597.
[33] F. Paonessa et al., "Recent results on the characterization of the LOFAR radio telescope by means of a micro UAV," in *Proc. 2017 Int. Conf. Electromagn. Adv Appl. (ICEAA)*, Verona, pp. 1752–1753. doi: 10.1109/ICEAA.2017.8065634.
[34] L. Ciorba et al., "Near-field phase reconstruction for UAV-based antenna measurements," in *Proc. 2019 13th Eur. Conf. Antennas Propagation (EuCAP)*, Krakow, Poland, pp. 1–4.
[35] S. F. Razavi and Y. Rahmat-Samii, "A new look at phaseless planar near-field measurements: Limitations, simulations, measurements, and a hybrid solution," *IEEE Antennas Propag. Mag.*, vol. 49, no. 2, pp. 170–178, Apr. 2007. doi: 10.1109/MAP.2007.376625.
[36] F. Rodríguez Varela, B. G. Iragüen, and M. Sierra-Castañer, "Application of nonuniform FFT to spherical near-field antenna measurements," *IEEE Trans. Antennas Propag.*, vol. 68, no. 11, pp. 7571–7579, Nov. 2020. doi: 10.1109/TAP.2020.2998898.
[37] M. A. Salari, O. Manoochehri, A. Darvazehban, and D. Erricolo, "An active 20-MHz to 2.5-GHz UWB receiver antenna system using a TEM horn," *IEEE Antennas Wireless Propag. Lett.*, vol. 16, pp. 2432–2435, 2017. doi: 10.1109/LAWP.2017.2723318.
[38] A. Darvazehban, O. Manoochehri, M. A. Salari, P. Dehkhoda, and A. Tavakoli, "Ultra-wideband scanning antenna array with Rotman lens," *IEEE Trans. Microw. Theory Techn.*, vol. 65, no. 9, pp. 3435–3442, Sept. 2017. doi: 10.1109/TMTT.2017.2666810.
[39] P. Busch, "Why clean spectrum is so important?" in *Proc. Rohde und Schwarz MNT Forum*, Oct. 2019. [Online]. Available: https://cdn.rohde-schwarz.com.cn/pws/dl_downloads/dl_common_library/dl_brochures_and_datasheets/pdf_1/MNT_Agenda_2019__final.pdf
[40] X. Lin et al., "The sky is not the limit: LTE for unmanned aerial vehicles," *IEEE Commun. Mag.*, vol. 56, no. 4, pp. 204–210, Apr. 2018. doi: 10.1109/MCOM.2018.1700643.
[41] T. S. Rappaport, Y. Xing, G. R. MacCartney, A. F. Molisch, E. Mellios, and J. Zhang, "Overview of millimeter wave communications for fifth-generation (5G) wireless networks—with a focus on propagation models," *IEEE Trans. Antennas Propag.*, vol. 65, no. 12, pp. 6213–6230, Dec. 2017. doi: 10.1109/TAP.2017.2734243.
[42] M. F. Ahmed, E. M. Naveed, P. Nar, and S. K. Jindal, "Design of an autonomous drone for IoT deployment analysis," in *Proc. 2019 Int. Conf. Vision Towards Emerging Trends Commun. Netw. (ViTECoN)*, Vellore, India, pp. 1–4. doi: 10.1109/ViTECoN.2019.8899609.
[43] L. Lo Monte, D. Erricolo, F. Soldovieri, and M. C. Wicks, "Radio frequency tomography for tunnel detection," *IEEE Trans. Geosci. Remote Sens.*, vol. 48, no. 3, pp. 1128–1137, Mar. 2010. doi: 10.1109/TGRS.2009.2029341.
[44] L. Lo Monte, D. Erricolo, F. Soldovieri, and M. C. Wicks, "RF tomography for below-ground imaging of extended areas and close-in sensing," *IEEE Geosci. Remote Sens. Lett.*, vol. 7, no. 3, pp. 496–500, July 2010. doi: 10.1109/LGRS.2009.2039918.
[45] A. Moreira, P. Prats-Iraola, M. Younis, G. Krieger, I. Hajnsek, and K. P. Papathanassiou, "A tutorial on synthetic aperture radar," *IEEE Geosci. Remote Sens. Mag.*, vol. 1, no. 1, pp. 6–43, Mar. 2013. doi: 10.1109/MGRS.2013.2248301.
[46] Y. Rodriguez-Vaqueiro et al., "Array of antennas for a GPR system onboard a UAV," in *Proc. 2019 IEEE Int. Symp. Antennas Propagation USNC-URSI Radio Sci. Meeting*, Atlanta, GA, pp. 821–822. doi: 10.1109/APUSNCURSINRSM.2019.8889164.
[47] M. Garcia-Fernandez, Y. Alvarez-Lopez, F. Las Heras, A. Morgenthaler, and C. Rappaport, "Analysis of multistatic vehicle-drone ground penetrating radar configurations for mine detection," in *Proc. 2019 IEEE Int. Symp. Antennas Propagation USNC-URSI Radio Sci. Meeting*, Atlanta, GA, pp. 1637–1638. doi: 10.1109/APUSNCURSINRSM.2019.8888340.
[48] M. Garcia-Fernandez et al., "Autonomous airborne 3D SAR imaging system for subsurface sensing: UWB-GPR on board a UAV for landmine and IED detection," *Remote Sens.*, vol. 11, no. 20, pp. 2357, 2019. doi: 10.3390/rs11202357.
[49] M. Garcia-Fernandez et al., "GPR system onboard a UAV for non-invasive detection of buried objects," in *Proc. 2018 IEEE Int. Symp. Antennas Propagation USNC/URSI Nat. Radio Sci. Meeting*, Boston, pp. 1967–1968. doi: 10.1109/APUSNCURSINRSM.2018.8608907.
[50] M. Garcia-Fernandez et al., "UAV-mounted GPR for NDT applications," in *Proc. 2018 15th Eur. Radar Conf. (EuRAD)*, Madrid, pp. 2–5. doi: 10.23919/EuRAD.2018.8546594.
[51] M. Garcia Fernandez et al., "Synthetic aperture radar imaging system for landmine detection using a ground penetrating radar on board an unmanned aerial vehicle," *IEEE Access*, vol. 6, pp. 45,100–45,112, Aug. 2018. doi: 10.1109/ACCESS.2018.2863572.
[52] I. Catapano, G. Gennarelli, G. Ludeno, and F. Soldovieri, "Applying ground-penetrating radar and microwave tomography data processing in cultural heritage: State of the art and future trends," *IEEE Signal Process. Mag.*, vol. 36, no. 4, pp. 53–61, July 2019. doi: 10.1109/MSP.2019.2895121.
[53] F. Sabatino, "Quadrotor control: Modeling, nonlinear control design, and simulation," Master's thesis, KTH Electrical Engineering, Stockholm, Sweden, June 2015.
[54] L. Washburn, E. Romero, C. Johnson, B. Emery, and C. Gotschalk, "Measurement of antenna patterns for oceanographic radars using aerial drones," *J. Atmospheric Oceanic Technol.*, vol. 34, no. 5, pp. 971–981, 2017. doi: 10.1175/JTECH-D-16-0180.1.
[55] B. P. A. Rohman, M. B. Andra, H. F. Putra, D. H. Fandiantoro, and M. Nishimoto, "Multisensory surveillance drone for survivor detection and geolocalization in complex post-disaster environment," in *Proc. 2019 IEEE Int. Geosci. Remote Sens. Symp. (IGARSS 2019)*, Yokohama, Japan, pp. 9368–9371. doi: 10.1109/IGARSS.2019.8899804.